Thermodynamic Properties for R-404A¹

K. Fujiwara,^{2,3} S. Nakamura,² M. Noguchi²

- ¹ Paper presented at theThirteenth Symposium on Thermophysical Properties, June 22-27, 1997, Boulder, Colorado, U.S.A.
- ² Chemical Division, Daikin Industries, Ltd., 1-1 Nishi Hitotsuya, Settsu-shi, Osaka 566 Japan.
- ³ To whom correspondence should be addressed.

ABSTRACT

An 18-coefficient modified Benedict-Webb-Rubin equation of state has been developed for R-404A, a ternary mixture of 44% in mass of pentafluoroethane (R-125), 52% in mass of 1,1,1-trifluoroethane (R-143a), and 4% in mass of 1,1,1,2-tetrafluoroethane (R-134a). Correlations of bubble point pressures, dew point pressures, saturated liquid densities, and saturated vapor densities are also presented. This equation of state has been developed based on the reported experimental data of *PVT* properties, saturation properties, isochoric heat capacities by using a least squares fitting.

These correlations are effective in the temperature range from 250 K to the critical temperature. This equation of state is effective at pressures up to 15 MPa, densities to 1300 kgm⁻³, and temperatures from 250 K to 400 K. The thermodynamic properties except for the saturation pressures are calculated from this equation of state.

KEY WORDS: correlation; equation of state; R-125; R-134a; R-143a; R-404A; thermodynamic properties.

1. INTRODUCTION

R-502, an azeotropic mixture of 48.8% in mass of dichlorodifluoroethane (R-22) and 51.2% in mass of chloropentafluoroethane (R-115), had been widely used as a refrigerant in low-temperature refrigerators. This substance has not been supplied since 1996 according to the Montreal Protocol. R-507, an azeotropic mixture of 50% in mass of pentafluoroethane (R-125) and 50% in mass of 1,1,1-trifluoroethane (R-143a) has been considered as an alternative to R-502. R-404A, an ternary mixture of 44% in mass of R-125, 52% in mass of R-143a, and 4% in mass of 1,1,1,2-tetrafluoroethane (R-134a) has been also considered as an alternative to R-502.

We have correlated bubble point pressures, dew point pressures, saturated liquid densities, and saturated vapor densities for R-404A. We have also developed an equation of state for R-404A. The form is an 18-coefficient modified Benedict-Webb-Rubin equation of state proposed by Piao et al. [1]. The thermodynamic properties except for the saturation pressures are calculated from this equation of state.

2. EXPERIMENTAL

STUDY

The critical parameters were reported by Bouchot and Richon [2] and Nakamura et al. [3].

Bouchot and Richon [2] reported 7 bubble point pressures, 9 dew point pressures, 9 saturated liquid densities, and 9 saturated vapor densities at temperatures from 253 K to 333 K.

Bouchot and Richon [2] also reported 214 *PVT* properties at pressures from 0.1 MPa to 2.9 MPa, densities from 4 kgm⁻³ to 1223 kgm⁻³, and temperatures from 253 K to 333 K. Nakamura et al. [3] reported 119 measurements at pressures from 1.5 MPa to 15

MPa, densities from 47 kgm⁻³ to 1247 kgm⁻³, and temperatures from 263 K to 403 K. Nakamura et al. [3] also reported 43 measurements along 3 isochores in a range of temperatures from 345 K to 393 K, pressures from 3.7 MPa to 7.8 MPa, and densities from 486 kgm⁻³ to 493 kgm⁻³.

One isochoric heat capacity data was reported by Nakamura et al. [4] at a pressure of 3 MPa and temperature of 264 K.

3. CRITICAL PARAMETERS

The critical parameters of Nakamura et al. [3] were used in this study. The numerical values are given as follows:

$$P_c = 3.761 \pm 0.002 \text{MPa} \tag{1}$$

$$r_c = 490 \pm 2 \text{kg} \cdot \text{m}^{-3}$$
 (2)

$$T_{c} = 345.15 \pm 0.01 \text{K} \tag{3}$$

4. CORRELATIONS

The following bubble point pressure, P', correlation was developed.

$$\ln\left(\frac{P'}{P_{c}}\right) = \frac{T_{c}}{T} \left[a_{1}' \left(1 - \frac{T}{T_{r}}\right) + a_{2}' \left(1 - \frac{T}{T_{r}}\right)^{1.5} + a_{3}' \left(1 - \frac{T}{T_{r}}\right)^{3} + a_{4}' \left(1 - \frac{T}{T_{r}}\right)^{6} \right]$$
(4)

The numerical values of the coefficients are listed in Table I. Fig. 1 shows a comparison of the bubble point pressure values calculated from Eq. (4) with the experimental data. Eq. (4) represents the data of Bouchot and Richon [2] with a maximum deviation of -0.6% and a standard deviation of 0.3%.

The dew point pressure, P ", correlation was developed as follows:

$$\ln\left(\frac{P''}{P_{c}}\right) = \frac{T_{c}}{T} \left[a_{1} \left[1 - \frac{T}{T_{c}} \right] + a_{2} \left[1 - \frac{T}{T_{c}} \right]^{1.5} + a_{3} \left[1 - \frac{T}{T_{c}} \right]^{3} + a_{4} \left[1 - \frac{T}{T_{c}} \right]^{6} \right]$$
(5)

The numerical values of the coefficients are listed in Table I. Fig. 2 shows a comparison of the dew point pressure values calculated from Eq. (5) with the experimental data. Eq. (5) represents the data of Bouchot and Richon [2] with a maximum deviation of -0.9% and a standard deviation of 0.4%.

The following saturated liquid density, r', correlation was developed.

$$\frac{\Gamma'}{\Gamma_c} = 1 + b_1' \left(1 - \frac{T}{T_c} \right)^{0.318} + b_2' \left(1 - \frac{T}{T_c} \right)^{2/3} + b_3' \left(1 - \frac{T}{T_c} \right) + b_4' \left(1 - \frac{T}{T_c} \right)^{4/3}$$
 (6)

The numerical values of the coefficients are listed in Table I. Fig. 3 shows a comparison of the saturated liquid density values calculated from Eq. (6) with the experimental data. Eq. (6) represents the data of Bouchot and Richon [2] within $\pm 0.2\%$.

The saturated vapor density, r ", correlation was developed as follows.

$$\frac{\Gamma''}{\Gamma_{c}} = 1 + b_{1} \left[\left(1 - \frac{T}{T_{c}} \right)^{0.318} + b_{2} \left[\left(1 - \frac{T}{T_{c}} \right)^{2/3} + b_{3} \left[\left(1 - \frac{T}{T_{c}} \right) + b_{4} \left[\left(1 - \frac{T}{T_{c}} \right)^{4/3} \right] \right] + b_{5} \left[\left(1 - \frac{T}{T_{c}} \right)^{3} + b_{6} \left[\left(1 - \frac{T}{T_{c}} \right)^{6} \right] \right]$$

$$(7)$$

The numerical values of the coefficients are listed in Table I. Fig. 4 shows a comparison of the saturated vapor density values calculated from Eq. (7) with the experimental data. Eq. (7) represents the data of Bouchot and Richon [2] with a maximum deviation of 1.3% and a standard deviation of 0.6%.

The coefficients of the following ideal-gas heat capacity, C_p° , equation were determined using those of the equations for R-125, R-134a, and R-143a reported by McLinden et al. [5].

$$\frac{C_{p}^{\circ}}{R} = c_{1} + c_{2} \frac{T}{T_{c}} + c_{3} \left(\frac{T}{T_{c}}\right)^{2} + c_{4} \left(\frac{T}{T_{c}}\right)^{3}$$
 (8)

where $R = 8.314471 \text{ kJkg}^{-1}\text{K}^{-1}$. The numerical values of the coefficients are given in Table I.

5. EQUATION OF STATE

Equations of state for mixtures are generally composed of equations of state for each components and mixing rules. Equations of state for each components with a large number of coefficients are used to meet the required accuracy of properties. On the other hand, mixing rules to apply these kinds of equations of state for mixtures are empirically developed. A large number of experimental data are required for each components as well as for mixtures. In the case that an equation of state obtained for a mixture dose not represent experimental data in the vapor-liquid equilibrium state very well, another equation of state and mixing rules for the vapor-liquid equilibrium state has to be developed.

We have developed an equation of state for R-404A without mixing rules because this equation of state mainly gives the thermodynamic properties in the single phase. The saturation pressures are calculated from correlations which are given as a function of temperature. The saturated densities are obtained as points where the isotherms of this equation of state and these saturation pressure correlations intersect.

The form of the equation of state in this study is an 18-coefficient modified Benedict-Webb-Rubin (MBWR) equation of state proposed by Piao et al. [1]. The equation of state is given as follows:

$$P_{\rm r} = \frac{T_{\rm r} \cdot \Gamma_{\rm r}}{Z_{\rm c}} + \sum_{\rm i=1}^{14} d_{\rm i} \cdot \frac{\Gamma_{\rm r}^{m_{\rm i}}}{T_{\rm r}^{n_{\rm i}}} + \sum_{\rm i=15}^{18} d_{\rm i} \cdot \frac{\Gamma_{\rm r}^{m_{\rm i}+3}}{T_{\rm r}^{n_{\rm i}}} \cdot \exp(-\Gamma_{\rm r}^{2})$$
(9)

where
$$P_{\rm r} = \frac{P}{P_{\rm c}}$$
, $\Gamma_{\rm r} = \frac{\Gamma}{\Gamma_{\rm c}}$, $T_{\rm r} = \frac{T}{T_{\rm c}}$, $Z_{\rm c} = \frac{P_{\rm c}M}{R\Gamma_{\rm c}T_{\rm c}}$, $M = 97.604 \,\mathrm{kg}\cdot\mathrm{kmol}^{-1}$,

 $R = 8.314471 \text{kJ} \cdot \text{kmol}^{-1} \cdot \text{K}^{-1}$. The coefficients are listed in Table II.

The present equation of state has been developed based on the reported experimental data of *PVT* properties, saturation properties, isochoric heat capacities by using a least squares fitting.

The Helmholtz free energy function, A, derived from Eqs. (8) and (9) is given as follows:

$$A_{\rm r} = \frac{A}{T_{\rm c} R Z_{\rm c}} = A_{\rm r}^{*} + A_{\rm r}^{\circ}$$
 (10)

where A_{r} is given below,

$$A_{r}^{*} = \sum_{i=1}^{14} d_{i} \cdot \frac{1}{m_{i} - 1} \cdot \frac{\Gamma_{r}^{m_{i} - 1}}{T_{r}^{n_{i}}} + \sum_{i=15}^{16} d_{i} \cdot \frac{1}{2} \cdot \frac{1}{T_{r}^{n_{i}}} \cdot \left[1 - \exp(-\Gamma_{r}^{2})\right] + \sum_{i=17}^{18} d_{i} \cdot \frac{1}{2} \cdot \frac{1}{T_{r}^{n_{i}}} \left[1 - \left(1 + \Gamma_{r}^{2}\right) \exp(-\Gamma_{r}^{2})\right] + \frac{T_{r}}{Z_{r}} \cdot \ln(\Gamma_{r})$$
 (11)

On the other hand, $A_{\rm r}$ is expressed as follows:

$$A_{\rm r}^{\circ} = U_{\rm r}^{\circ} - T_{\rm r} S_{\rm r}^{\circ} \tag{12}$$

where

$$U_{r}^{\circ} = \frac{1}{Z_{c}} \left[\left(c_{1} - 1 \right) \left(T_{r} - T_{r}^{\circ} \right) + \frac{c_{2}}{2} \left(T_{r}^{2} - T_{r}^{\circ 2} \right) + \frac{c_{3}}{3} \left(T_{r}^{3} - T_{r}^{\circ 3} \right) + \frac{c_{4}}{4} \left(T_{r}^{4} - T_{r}^{\circ 4} \right) + c_{u} \right]$$

$$\tag{13}$$

$$S_{\rm r}^{\circ} = \frac{1}{Z_{\rm c}} \left[\left(c_1 - 1 \right) \ln \frac{T_{\rm r}}{T_{\rm r}^{\circ}} + c_2 \left(T_{\rm r} - T_{\rm r}^{\circ} \right) + \frac{c_3}{2} \left(T_{\rm r}^2 - T_{\rm r}^{\circ 2} \right) + \frac{c_4}{3} \left(T_{\rm r}^3 - T_{\rm r}^{\circ 3} \right) + c_s \right]$$
(14)

where $T_{\rm r}^{\circ} = \frac{273.15}{T_{\rm c}}$. The two numerical constants, $c_{\rm u}$ and $c_{\rm s}$, are given so that the specific

enthalpy and entropy values at 273.15 K for the saturated liquid state are 200 kJkg⁻¹ and 1 kJkg⁻¹K⁻¹, respectively.

The enthalpy and entropy values are given in the following thermodynamic relation, respectively.

$$S_{\rm r} = \frac{S}{RZ_{\rm c}} = -\left(\frac{\P A_{\rm r}}{\P T_{\rm r}}\right)_{\rm r} \tag{15}$$

$$H_{\rm r} = \frac{H}{T_{\rm c}RZ_{\rm c}} = A_{\rm r} - T_{\rm r} \left(\frac{\P A_{\rm r}}{\P T_{\rm r}}\right)_{\rm r,r} + r_{\rm r} \left(\frac{\P A_{\rm r}}{\P r_{\rm r}}\right)_{T_{\rm r}}$$
(16)

The isochoric heat capacity, isobaric heat capacity, and speed of sound values are also given in the following thermodynamic relation, respectively.

$$\left(C_{v}\right)_{r} = \frac{C_{v}}{RZ_{c}} = -T_{r} \left(\frac{\P^{2}A_{r}}{\P T_{r}^{2}}\right)_{\Gamma_{r}}$$

$$\tag{17}$$

$$(C_{p})_{r} = \frac{C_{p}}{RZ_{c}} = T_{r} \left[-\left(\frac{\P^{2}A_{r}}{\P T_{r}^{2}}\right)_{\Gamma_{r}} + \frac{\Gamma_{r}\left(\frac{\P^{2}A_{r}}{\P T_{r}\P \Gamma_{r}}\right)^{2}}{2\left(\frac{\P A_{r}}{\P \Gamma_{r}}\right)_{T_{r}} + \Gamma_{r}\left(\frac{\P^{2}A_{r}}{\P \Gamma_{r}^{2}}\right)_{T_{r}}} \right]$$
 (18)

$$(W^{2})_{r} = \frac{W^{2}}{T_{c}RZ_{c}} = r_{r}^{2} \left[\frac{2}{r_{r}} \left(\frac{\P A_{r}}{\P r_{r}} \right)_{T_{r}} + \left(\frac{\P^{2}A_{r}}{\P r_{r}^{2}} \right)_{T_{r}} - \frac{\left(\frac{\P^{2}A_{r}}{\P T_{r} \P r_{r}} \right)^{2}}{\left(\frac{\P^{2}A_{r}}{\P T_{r}^{2}} \right)_{r_{r}}} \right]$$
 (19)

6. DISCUSSION

Fig. 5 shows a comparison of the single phase density values calculated from Eq. (9) with experimental data. The present equation of state represents the data of Bouchot and Richon [2] in the liquid state within 0.3% and in the vapor state with a maximum deviation of 4.3% and a standard deviation of 1.2%. The data at densities up to 150 kgm⁻

³ are represented within 0.5 kgm⁻³. This equation of state represents the data of Nakamura et al. [3] with a maximum deviation of 2.3% and a standard deviation of 0.4% except for the 43 measurements along 3 isochores: 487 kgm⁻³; 490 kgm⁻³; 493 kgm⁻³. These 43 data are represented by the present equation of state within 0.5% in pressure.

Fig. 6 shows a comparison of the saturated liquid density values calculated from Eqs. (4), and (9) with the experimental data. The present equation of state represents the data of Bouchot and Richon [2] within 0.2%

Fig. 7 shows the comparison of the saturated vapor density values calculated from Eqs. (5) and (9) with the experimental data. The present equation of state represents the data of Bouchot and Richon [2] with a maximum deviation of 1% and a standard deviation of 0.5%.

The isochoric heat capacity value of Nakamura et al. [4] in the liquid state is represented by Eq. (17) with a deviation of -2.8%.

Figs. 8, 9, and 10 show the isochoric heat capacity, isobaric heat capacity and speed of sound values calculated from Eqs. (17), (18), and (19), respectively. These isobars show consistent behavior from the thermodynamic point of view between 220 K and 540 K.

7. CONCLUSION

An 18-coefficient MBWR equation of state for R-404A has been developed. Correlations of bubble point and dew point pressures and of saturated liquid and vapor densities are also presented. These correlations are considered to be effective at temperatures from 250 K to the critical temperature. This equation is considered to be effective in the range of temperatures from 250 K to 400 K, densities up to 1300 kgm⁻³, and pressures up to 15 MPa. This equation of state gives the thermodynamic properties

except for the saturation pressures.

REFERENCES

- 1. C.-C. Piao, M. Noguchi, H. Sato, and K. Watanabe, ASHRAE Transactions V. 100, Pt. 1: 3771 (1994).
- 2. C. Bouchot and D. Richon, 19th International Congress of Refrigeration, Hague, the Netherlands (1995).
- 3. S. Nakamura, K. Fujiwara, and M. Noguchi, 1996 JAR Annual Conference, Fukuoka, Japan (1996).
- 4. S. Nakamura, K. Fujiwara, C.-C. Piao, and M. Noguchi, 17th Japan Symposium of thermophysical Properties, Tsukuba, Japan (1996).
- 5. M. O. McLinden, M. L. Huber, and S. L. Outcalt, ASME Winter Annual Meeting, New Orleans, Louisiana (1993).

Table I. Coefficients of Eqs. (4), (5), (6), (7), and (8)

i	a_{i}	a_i ,	$b_{ m i}$	$b_{ m i}$,,	$c_{ m i}$
1	-7.37917	-7.59385	0.963411	-2.13109	2.60716
2	1. 269	1.77079	5.68670	2.14542	9.41515
3	46	-3.71716	-10.2368	-4.61060	-0.325675
4	-1.64715	3.24320	7.23707	4.67897	-0.547398
5	-7.12355			-1.67211	
6				1.01657	

Table II. Coefficients of Eq. (9) and constants, $c_{\rm u}$ and $c_{\rm s}$

i	$m_{ m i}$	$n_{ m i}$	$d_{ m i}$
1	2	-1	1.96433581401
2	2	0	-3.56987977471
3	2	2	-3.71200450596
4	2	3	-0.0926720977755
5	3	-1	2.45744505455
6	3	0	-4.50853991488
7	3	2	5.17635519994
8	4	0	-0.313494002253
9	4	2	-1.08476103077
10	5	0	1.61429976497
11	5	1	-0.848565739838
12	6	0	-0.516634795318
13	6	1	0.145585376781
14	7	0	0.109212328026
15	0	0	0.504178247791
16	0	1	0.702360275972
17	2	0	-0.606504041978
18	2	1	1.25624780433
C _u			12.1997905929
C _s			16.4589008290

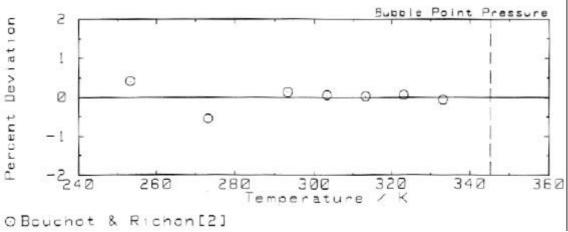


Fig. 1. Comparison of the bubble point pressure values calculated from Eq. (4) with the experimental data.

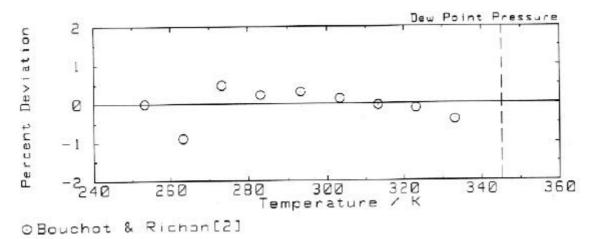


Fig. 2. Comparison of the dew point pressure values calculated from Eq. (5) with the experimental data.

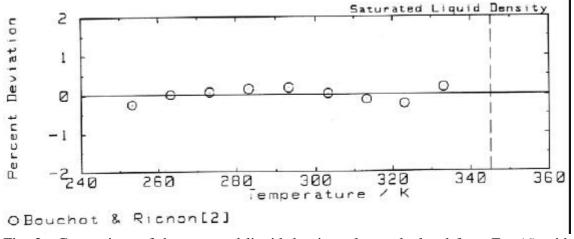


Fig. 3. Comparison of the saturated liquid density values calculated from Eq. (6) with the experimental data.

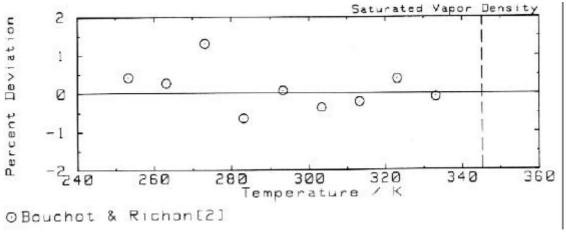


Fig. 4. Comparison of the saturated vapor density values calculated from Eq. (7) with the experimental data.

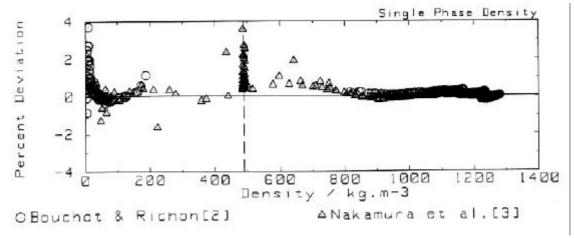


Fig. 5. Comparison of the single-phase density values calculated from Eq. (9) with the experimental data.

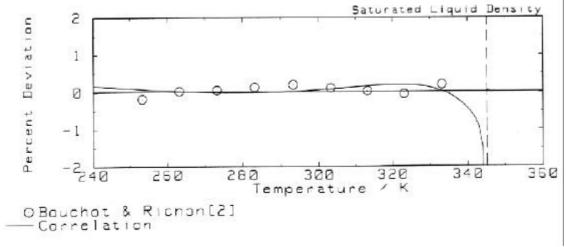


Fig. 6. Comparison of the saturated liquid density values calculated from Eqs. (4) and (9) with the experimental data.

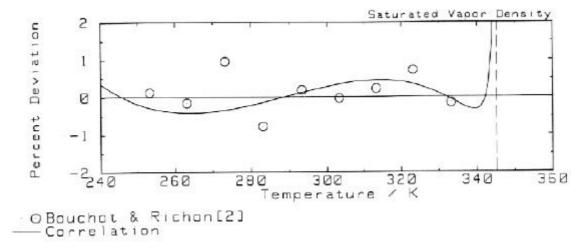


Fig. 7. Comparison of the saturated vapor density values calculated from Eqs. (5) and (9) with the experimental data.

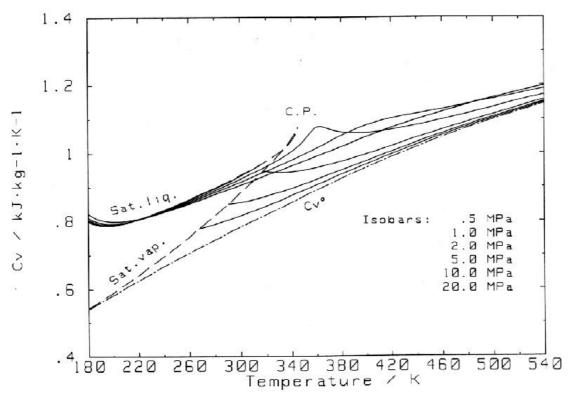


Fig. 8. Isochoric heat capacity values calculated from Eq. (17).

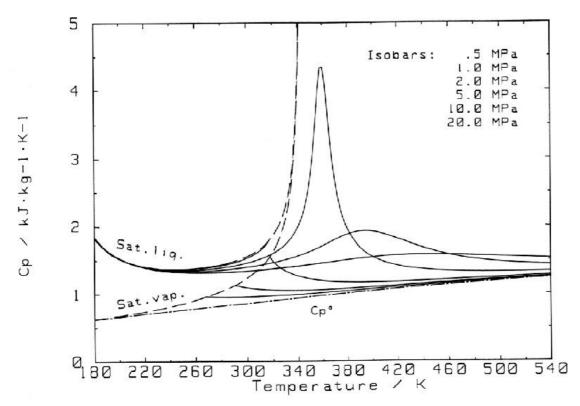


Fig. 9. Isobaric heat capacity values calculated from Eq. (18).

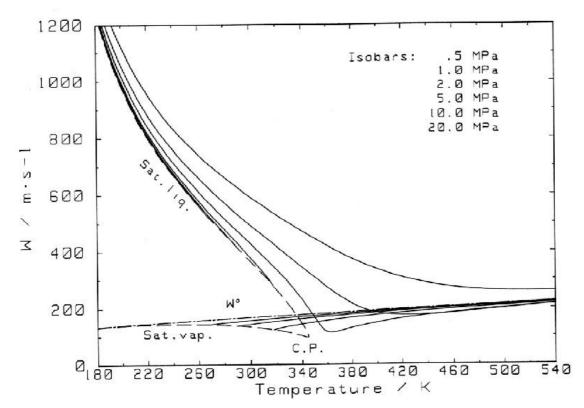


Fig. 10. Speed of sound values calculated from Eq. (19).